You might find this additional information useful...

This article cites 56 articles, 25 of which you can access free at:
http://jn.physiology.org/cgi/content/full/96/3/1602#BIBL

Updated information and services including high-resolution figures, can be found at:
http://jn.physiology.org/cgi/content/full/96/3/1602

Additional material and information about *Journal of Neurophysiology* can be found at:
http://www.the-aps.org/publications/jn

This information is current as of August 15, 2006 .

Encoding of Naturalistic Optic Flow by a Population of Blowfly Motion-Sensitive Neurons

K. Karmeier,[1] J. H. van Hateren,[2] R. Kern,[1] and M. Egelhaaf[1]

[1]*Department of Neurobiology, Faculty for Biology, Bielefeld University; Bielefeld, Germany; and* [2]*Department of Neurobiophysics, University of Groningen, Groningen, The Netherlands*

Karmeier, K., J. H. van Hateren, R. Kern, and M. Egelhaaf.
Encoding of naturalistic optic flow by a population of blowfly
motion-sensitive neurons. *J Neurophysiol* 96: 1602–1614, 2006.
First published May 10, 2006; doi:10.1152/jn.00023.2006. In sensory systems information is encoded by the activity of populations of
neurons. To analyze the coding properties of neuronal populations
sensory stimuli have usually been used that were much simpler than
those encountered in real life. It has been possible only recently to
stimulate visual interneurons of the blowfly with naturalistic visual
stimuli reconstructed from eye movements measured during free
flight. Therefore we now investigate with naturalistic optic flow the
coding properties of a small neuronal population of identified visual
interneurons in the blowfly, the so-called VS and HS neurons. These
neurons are motion sensitive and directionally selective and are
assumed to extract information about the animal's self-motion from
optic flow. We could show that neuronal responses of VS and HS
neurons are mainly shaped by the characteristic dynamical properties
of the fly's saccadic flight and gaze strategy. Individual neurons
encode information about both the rotational and the translational
components of the animal's self-motion. Thus the information carried
by individual neurons is ambiguous. The ambiguities can be reduced
by considering neuronal population activity. The joint responses of
different subpopulations of VS and HS neurons can provide unambiguous information about the three rotational and the three translational components of the animal's self-motion and also, indirectly,
about the three-dimensional layout of the environment.

INTRODUCTION

Even single aspects of the world, such as the orientation of
contours or the frequency of a tone, induce an activity pattern
spread over multiple neurons. A given environmental situation,
such as the movements of an animal in its environment, is
reflected in this neuronal population activity rather than in the
responses of single neurons. Population coding of sensory
information has been analyzed in many studies (e.g., Averbeck
and Lee 2004; Deadwyler and Hampson 1997; Nirenberg and
Latham 1998; Pouget et al. 2000). The sensory input an animal
encounters in real life, however, may have much more complex
properties than the experimenter-defined stimuli usually used
in these studies (for review see Reinagel 2001).

We analyze the coding properties of a population of motion-sensitive visual interneurons in the blowfly with naturalistic
stimuli generated actively by the animal during nearly unrestrained behavior. This neuronal population consists of two
classes of neurons, the 10 VS (vertical system) neurons (Heng-
stenberg 1982; Hengstenberg et al. 1982; Krapp et al. 1998)
and the three HS (horizontal system) neurons (Hausen
1982a,b) whose response properties and function in visually
guided behavior have been characterized in great detail (for
reviews see Borst and Haag 2002; Egelhaaf et al. 2002, 2004).
HS neurons are excited primarily by front-to-back motion and
their receptive fields jointly cover one visual hemisphere. The
latter is also true for VS neurons, which are most sensitive to
downward motion within a vertical stripe of the visual field
(Fig. 1*A*). Based on their receptive field properties (Krapp et al.
1998, 2001) and their synaptic connections, all VS and HS
neurons were proposed to act mainly as rotation sensors (Farrow et al. 2005; Haag and Borst 2001, 2004; Horstmann et al.
2000; Krapp et al. 2001).

This view was challenged recently when two individual
neurons, the HSE and the H1, were stimulated with the retinal
image motion encountered by freely flying flies (Boeddeker et
al. 2005; Kern et al. 2005; van Hateren et al. 2005). These
neurons could be demonstrated to make use of the saccadic
flight strategy of freely flying flies, where most rotational
self-motion is squeezed into brief periods of high rotation
velocity, the saccades. Between saccades *1*) the gaze is kept
basically straight (Schilstra and van Hateren 1999; van Hateren
and Schilstra 1999) and *2*) both neurons provide information
about rotational and translational self-motion and thus indirectly about the three-dimensional (3D) structure of the environment (Kern et al. 2005; van Hateren et al. 2005). These
studies revealed that the coding properties of visual interneurons under natural stimulus conditions are not easily predictable from results of studies using conventional experimenter-defined stimuli.

Here, we characterize for the first time almost the entire
population of VS and HS neurons, representing the major
motion-sensitive output neurons of the blowfly visual system,
with naturalistic retinal image motion. We will demonstrate
that all three rotational and translational self-motion components can be decoded from appropriately combined responses
of different VS and HS neurons, if the specific retinal image
motion as actively generated by the fly in free-flight maneuvers
is taken into account.

METHODS

Visual stimulation

The position and orientation of the head of blowflies (*Calliphora
vicina*) flying in a cage of about $40 \times 40 \times 40$ cm^3 were recorded
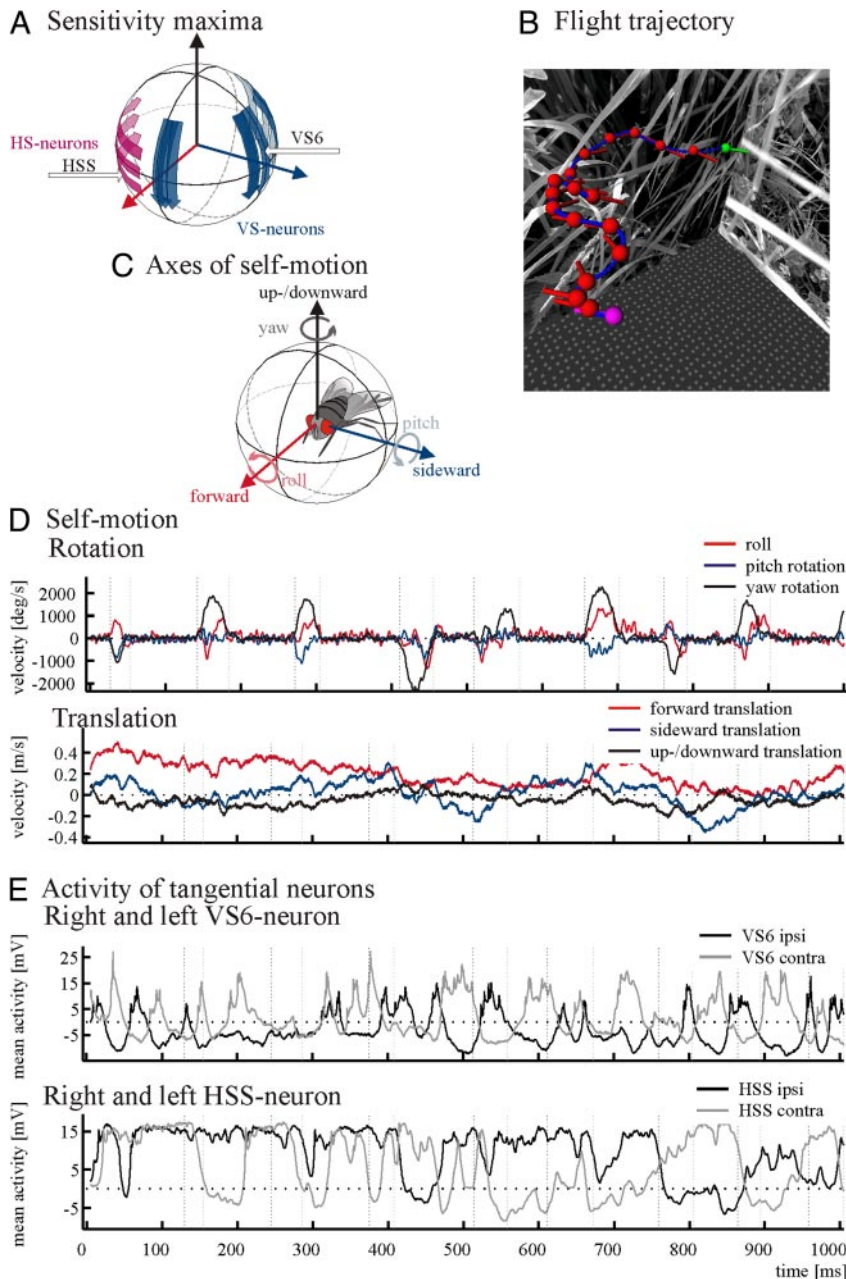
FIG. 1. Response characteristics of tangential neurons during stimulation with behaviorally generated optic flow. *A*: areas of main sensitivity to motion of fly tangential neurons. VS (vertical system) neurons (shown for the left side of the brain) are depolarized by downward motion, HS (horizontal system) neurons (shown for the right side of the brain) by front-to-back motion in the most sensitive parts of their receptive fields. Maximum sensitivities of VS neurons are distributed from the frontal (VS1) to the caudal part of the visual hemisphere (VS10). Sensitivity maximum of the HSS neuron is located in the ventral part of the visual field; the HSE neuron is most sensitive to motion in the equatorial and the HSN neuron in the dorsal part of the visual field. *B*: 1-s section of a fly's trajectory (blue line) in a side view in a cage of about $40 \times 40 \times 40$ cm³. Position and orientation of the head are shown every 50 ms (red dots; green and magenta dots indicate respectively the start and end points of the flight sequence). *C*: self-motion of the fly can be decomposed into rotational (roll, pitch, yaw) and translational components (forward, sideward, upward/downward velocity) around/along the 3 cardinal head axes (frontal, transverse, vertical). *D*: head rotation (*top*) and translation velocity (*bottom*) during the flight segment shown in *B*. Rotation and translation around/along the frontal head axis (roll, forward velocity) in red, rotation and translation around/along the transverse head axis (pitch, sideward velocity) in blue, rotation and translation around/along the vertical head axis (yaw, upward/downward velocity) in black. Positive velocities denote leftward movements. As a visual aid for comparing the traces, black and gray dotted vertical lines indicate the beginning and end of saccades. *E*: average membrane potential of tangential neurons. *Top*: ipsi- and contralateral VS6 neuron (mean over *4–5 traces*). *Bottom*: ipsi- and contralateral HSS neuron recorded from another animal (mean over *3 traces*). Response of the ipsilateral neurons was measured directly, and their response to appropriately mirrored versions of the movies provided an approximation of the response of the contralateral neurons. Resting potential was set to zero (dotted horizontal line); *neuronal response traces* were shifted back in time by 22.5 ms to account for response latencies. Vertical lines as in *D*.

using magnetic fields driving search coils attached to the flies' head (Schilstra and van Hateren 1999; van Hateren and Schilstra 1999). Because the compound eye is an integral part of the head, and the spatial coordinates of the head and the visual interior of the cage are known, we could use the head trajectory to reconstruct the visual stimulus encountered by the fly during its flight (Fig. 1*B*; Lindemann et al. 2003). Reconstructions of 10 flights of 3.45-s duration each, originating from three different flies, were used in the present measurements. Stimuli were presented using FliMax, a special-purpose panoramic stimulus device that generates image frames at a frequency of 370 Hz (Lindemann et al. 2003). Each of the stimulus movies resulting from the reconstruction was accompanied by a "no translation" variant (called "NT" below), reconstructed from the rotational movements (yaw, roll, and pitch) of the flies only, whereas their position was fixed to the center of the cage. During a recording we presented the normal and the mirrored version of a movie, thus obtaining the response of the ipsilateral neuron and an approximated response of its contralateral counter-

part. This response will be referred to in the following as the response of the contralateral neuron.

Electrophysiology

Experiments were done on 1- to 2-day-old female blowflies (*Calliphora vicina*) bred in our laboratory stock. The dissection of the animals for electrophysiological experiments followed standard procedures described elsewhere (Warzecha et al. 1993). The flies' eyes were aligned with the stimulus device according to the symmetrical deep pseudopupil (Franceschini 1975). Intracellular recordings from VS and HS neurons in the right lobula plate (third visual neuropile) were made using borosilicate electrodes (GC100TF10, Clark Electromedical) pulled on a Brown-Flaming puller (P-97, Sutter Instruments). Electrodes were filled with 1 M KCl and had resistances between 20 and 40 MΩ. Recordings were carried out using standard electrophysiology equipment. The data were low-pass filtered (corner frequency 2.4 kHz) and sampled at a rate of 4 kHz (I/O-card DT3001,

Data Translation) using the VEE Pro 5.0 (Agilent Technologies) in conjunction with DT VPI (Data Translation) software. Experiments were done at temperatures between 28 and 32°C. Such relatively high temperatures closely approximate the fly's head temperature during flight (Stavenga et al. 1993). VS and HS neurons were identified by the location of their receptive field, their preferred direction of motion, and their signal structure (Hausen 1982a,b; Hengstenberg 1982; Krapp et al. 1998).

Data analysis

SELF-MOTION COMPONENTS. We calculated the coherence between neuronal responses and each of the six parameters of self-motion. Three of the self-motion parameters are rotational: yaw, pitch, and roll velocity; and the other three are translational: forward, sideward, and upward/downward velocity (Fig. 1*C*). The yaw velocity of the head is the instantaneous angular velocity around a vertical axis through the head and is obtained from the differential rotation matrix in the coordinate system of the head (Schilstra and van Hateren 1999; van Hateren and Schilstra 1999). Pitch and roll are rotations around transverse and frontal axes through the head, respectively. The forward, sideward, and upward/downward velocity of the head are the velocity components along frontal, transverse, and vertical axes through the head, respectively. We found that typically only a few of these parameters gave coherences >0.1 for a particular type of neuron.

COHERENCE CALCULATION. The coherence between a certain self-motion parameter of the fly (e.g., yaw velocity) and the neuronal response was calculated as $\gamma_b^2(\omega) = |P_{sr}(\omega)|^2/[P_{ss}(\omega)P_{rr}(\omega)]$ (Haag and Borst 1998; Theunissen et al. 1996; van Hateren and Snippe 2001), where P_{sr} is the cross-spectral density of self-motion velocity and response, P_{ss} is the power spectral density of the self-motion velocity and P_{rr} is that of the response, and $\omega = 2\pi f$, where f is frequency. Spectra were calculated by periodogram averaging of 50% overlapping data segments, with each periodogram being the discrete Fourier transform of a $\cos^2$-tapered zero-mean data segment of 256 ms, extended by zero-padding to 512 ms. Results were not strongly dependent on segment length. Before segmentation, the response was aligned with the stimulus by shifting it 22.5 ms backward in time, the approximate latency under the experimental conditions. Results were not strongly dependent on shift size. Segments from all flights (between one and ten) used as stimulus for a particular neuron were included in the periodogram averaging. Bias in the coherence estimate of each stimulus repetition was corrected by $\gamma^2 = [n/(n-1)\gamma_b^2] - 1/(n-1)$ (van Hateren and Snippe 2001; van Hateren et al. 2002), where n is the number of segments ($n = 25–250$ for the one to ten flights of the present experiments). Coherences were finally averaged over all stimulus repetitions.

COHERENCES WITH MORE THAN ONE PARAMETER. The coherence between the response and a second self-motion parameter was obtained by first conditioning the second parameter with the first (Bendat and Piersol 2000), i.e., $s_2'(\omega) = s_2(\omega) - [P_21(\omega)/P_{11}(\omega)]s_1(\omega)$, where $s_1(\omega)$ is the first parameter (e.g., Fourier transform of yaw velocity) and $s_2(\omega)$ and $s_2'(\omega)$ are, respectively, the original and conditioned second parameters (e.g., Fourier transform of sideward velocity); P_{21} and P_{11} are cross- and power spectra of the second and first parameters. Conditioning removes from s_2 the second-order statistical dependency with s_1. With three stimulus parameters (e.g., yaw, sideward, and forward velocity; Fig. 3*B*), the conditioned third parameter is $s_3' = s_3 - (P_{32}/P_{2'2'})s_2' - (P_{31}/P_{11})s_1$, where the dependency on ω is omitted for simplicity of notation. This conditioning removes from s_3 the second-order statistical dependency with both s_1 and s_2'. We found for the parameters used in this study that the order of evaluating parameters does not significantly affect the coherences of each parameter.

COHERENCE IN INTERSACCADIC INTERVALS. The above method gives coherences for the entire response. These coherences may be strongly dominated by the saccades because at least rotational self-motion parameters are much larger during saccades than between saccades. To focus on the stimulus–response relationship between saccades, we constructed masks $m(t)$ for masking (i.e., zeroing) the saccadic part of the stimulus and response (Kern et al. 2005; van Hateren et al. 2005). We then calculated the coherence between a masked self-motion parameter $m(t)s(t)$ and the masked response $m(t)r(t)$, rather than between the self-motion parameter $s(t)$ and response $r(t)$ as above. Masks selecting intersaccadic segments were obtained by first constructing masks $m_s(t)$ selecting saccades. A mask $m_s(t)$ was obtained by giving it the value 1 in a region surrounding each saccade, and zero elsewhere. Saccades were detected from peaks (≥ 500°/s) in the total angular velocity of the head. The saccadic regions were made large enough to include all parts of both saccadic stimulus and corresponding response. Regions of saccades that were close together were merged to reduce boundary effects. Edges of the masks were tapered with a 12.5-ms $\cos^2$-taper to reduce spectral leakage biasing the coherence estimate at high frequencies. The mask used for selecting the intersaccadic segments, $m(t)$, is then defined as $m(t) = 1 - m_s(t)$. Masked data consisted of gated (transmitted) data intermitted with blocks of zeroes. Although the mask shapes the power and cross-spectra of the masked data, this shaping occurs in a similar way for all spectra in the numerator and denominator of the definition of coherence. Consequently, the mask by itself does not generate coherence for uncorrelated data, as was confirmed in control computations with uncorrelated noise. The coherence of masked data include the zero blocks, however, and therefore should be regarded as belonging to the entire masked signal, not to just its intersaccadic part.

COHERENCE RATE. For coherence functions a coherence rate (van Hateren and Snippe 2001; van Hateren et al. 2002) can be defined as $R_{coh} = -\int_O^{f_0} \log_2(1 - \gamma^2)\mathrm{d}f$, where f is frequency and f_0 represents a frequency sufficiently high such that the coherence has become zero (default 150 Hz in this study). The coherence rate is expressed in bit/s and can be considered as a biased information rate; it is equal to Shannon's information rate in the case of independent Gaussian signals and noise. The coherence rate is used here as a convenient way to assign a single number to the coherence function (van Hateren and Snippe 2001).

TUNING OF VS NEURONS. For an analysis of the tuning of VS neurons to the animal's self-rotation, we did not use the coherences to self-motion around only the cardinal body axes. We projected the actual head rotation onto axes of varying elevation and azimuth (azimuth between −180 and 175°, elevation between −90 and 85°, 5 ° steps). We then calculated the coherence rate between the neuronal response and this projected head rotation (Fig. 2*B*). The rotational axis (i.e., azimuth and elevation) that gave the maximum coherence rate was used as an estimate for the preferred rotation axis of the given VS neuron. For each neuron, such estimates were obtained for typically eight conditions (all combinations of normal and mirrored movie, original and NT stimulus version, and coherence of total or only intersaccadic response). The mean and SE of all estimates for a particular neuron are shown in Fig. 2, *C* and *D*.

CALCULATION OF THE MEAN COHERENCE. Instead of showing a large number of coherence functions for all groups of neurons and all conditions (normal and mirrored movie, original and NT stimulus version, and coherence of total or only intersaccadic response), we calculated a mean coherence by averaging over frequencies in a 10-Hz band around the frequency with maximum coherence. Because all neurons of a certain cell class (VS class or HS class) reveal a similar frequency dependency for a particular self-motion component and a particular stimulus condition (e.g., upward/downward translation or preferred rotation for the original stimulus), we determined the posi-

A Characterizing stimulus

C Orientation of preferred rotation axes

B VS6-neuron: rotation tuning

D Preferred rotation axes and sensitivity maxima

$$y = -1.1 * x + 84$$
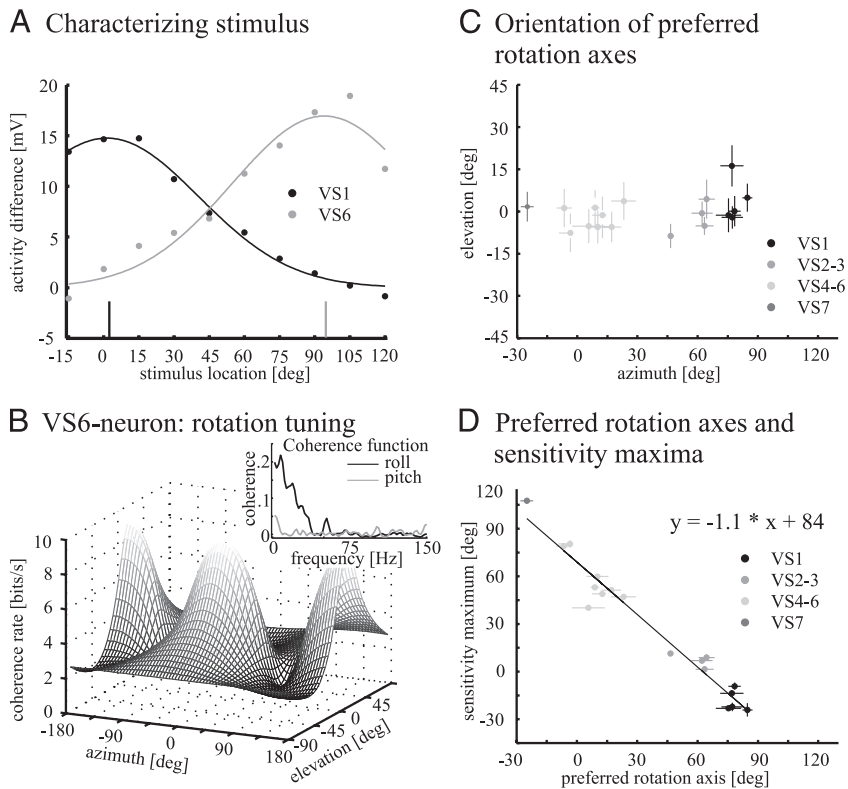
FIG. 2. Classification of VS neurons and determination of the respective preferred rotation axis. *A*: receptive field as determined by the difference between the neuronal responses to an up- and downward moving dot for a VS1 and a VS6 neuron. Difference responses are plotted as a function of the stimulus positions along the azimuth. Gaussian functions are fitted to the measured data of the 2 neurons. Arrows pointing at the *x*-axis denote the maximum of the fits and can be regarded as the sensitivity maximum of the respective neurons. *B*: tuning curve of the VS6 neuron to rotation obtained from the coherence rate. *Inset*: coherence functions between the VS6 neuron's response and the roll and pitch velocity. Coherence rate was calculated from the coherence function over a frequency range from 1 to 150 Hz. To obtain the tuning curve, the coherence rate was calculated for head rotations around axes in a 2-D grid. Azimuth between −180 (roll-axis) and 175°, elevation between −90 and 85° (5° steps). Azimuth value of −90/90° corresponds to the pitch axis. *C*: azimuth and elevation of the average preferred rotation axes for all VS neurons recorded in the experiments. An average axis and corresponding SE were calculated by weighting the axis for each stimulus condition, obtained from the peak of a tuning curve as presented in *B*, with the coherence rate at the respective peak. *D*: preferred rotation axes as a function of receptive fields' sensitivity maxima calculated as shown in *A* (mean and SE). Linear regression line fitted to the data has a slope of −1.1.

tion of the frequency band from the coherence averaged over all neurons belonging to that VS or HS class.

RESULTS

Flight description

The stimuli used in this study are reconstructed from the image flow blowflies experienced during free flight in a cage. Figure 1*B* shows as an example a 1,000-ms section of a flight trajectory. The head position (red dots) and orientation of the fly are shown every 50 ms. Flights can be described as a rapid succession of two phases, saccades and intersaccadic intervals. During "saccades" the fly shifts its gaze rapidly by fast head and body turns, whereas between saccades the gaze is kept relatively stable. This gaze strategy becomes particularly obvious, if the fly's self-rotation is decomposed into rotations around the three cardinal axes of the head (frontal, transverse, and vertical; Fig. 1, *B* and *D*, *top*). A saccade is characterized by rotations around all three axes. As an aid to comparing the stimulus and response traces in the figure, the approximate position of each saccade is marked by vertical lines at its beginning (black) and end (gray). The angular motions during saccades are dominated by rotations around the vertical axis that reach velocities of up to a few thousand degrees per second (yaw; black). Rotations around the transverse (pitch; blue) and the frontal axes (roll; red) are smaller and reach only about 1,000°/s. Between saccades the rotation velocities of the head around all three axes are by at least one order of magnitude smaller and are typically <200°/s (van Hateren and Schilstra 1999). In contrast to the rotational velocities, the time course of the translational velocity components is not structured in a similar way by the saccades. Rather, the translation velocities vary relatively smoothly and show no consistent changes

during the saccades [Fig. 1*D*, *bottom*; forward (red), sideward (blue), and upward/downward (black) velocities]. The forward velocity for the flight segment shown in Fig. 1*B* varies between 0 and 0.5 m/s. In other sections of the flights used it reaches ≤1 m/s (Schilstra and van Hateren 1999). The sideward and upward/downward velocities fluctuate around 0 m/s. For all flights, both the sideward and the upward/downward motion reach maximum velocities of about 0.5 m/s.

Responses of tangential neurons to naturalistic optic flow

Figure 1*E* shows the time course of averaged responses of an ipsilateral VS6 neuron (black line, *top*) and of an HSS neuron (black line, *bottom*) as well as the responses inferred for the respective contralateral neurons (gray). The responses were recorded from a blowfly watching the movie reconstructed from the flight shown in Fig. 1*B*. Both types of neurons respond with graded changes of their membrane potential to the naturalistic optic flow. The activity of both VS6 neurons modulates considerably around the resting potential (set to zero). For large parts of the flight the membrane potential modulations of the ipsi- and contralateral VS6 neuron appear to be in counterphase. It is hard to relate the responses to any single self-motion parameter. In particular, pronounced de- and hyperpolarizations are induced not only by the high rotation velocities during saccades but also in the intersaccadic intervals. Because the most obvious changes of translation velocity appear to occur on a slower timescale than most rotational velocity changes, the membrane potential changes, in particular between saccades, may be also related to the translational flow component. At first sight, these results on the VS6 neuron appear to be in contrast to results obtained with simple experimenter-defined stimuli, where this neuron was concluded to be
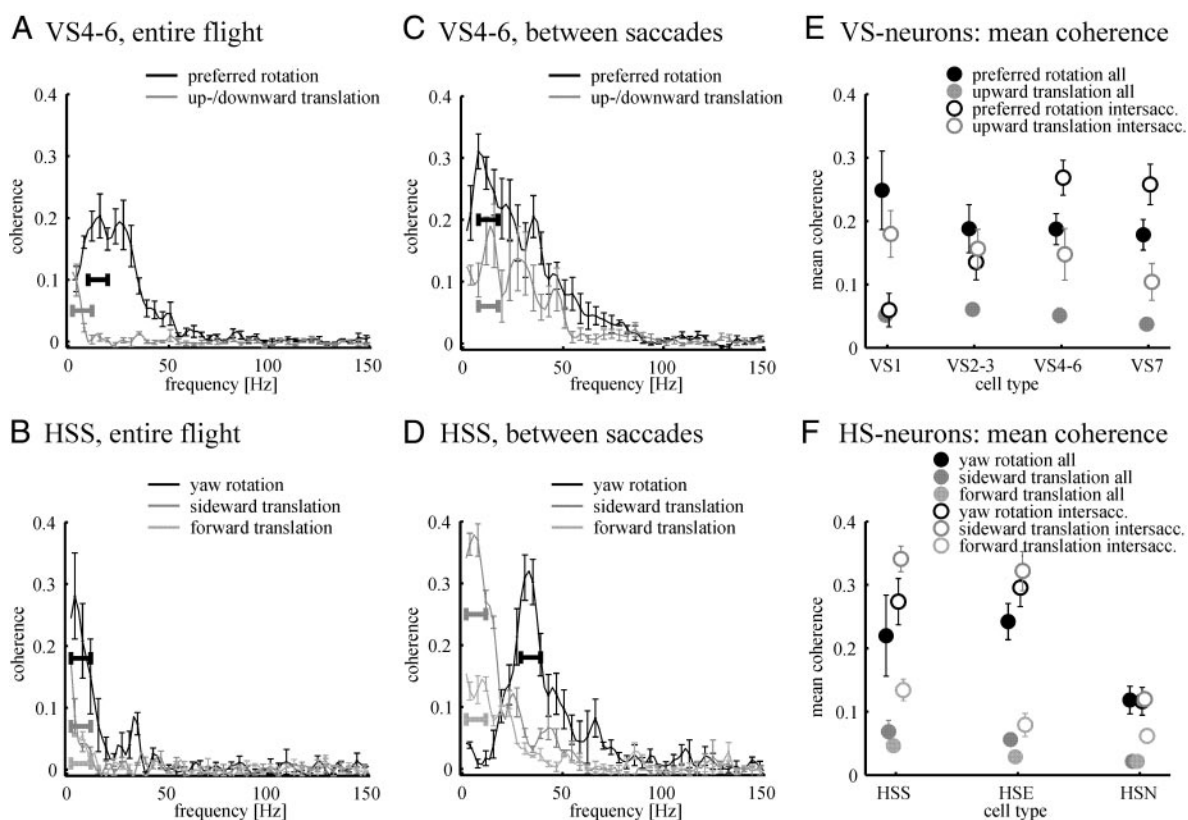
FIG. 3. Coherences between responses of tangential neurons and rotational or translational velocities. *A*: mean and SE of the coherence between the response (entire flight) of each VS4-6 neuron and the rotational velocity around its preferred rotation axis, and coherence with upward/downward velocity. Preferred rotation axis was obtained from the tuning curve calculated from coherence rates (cf. Fig. 2*B*). Horizontal bars in *A–D* denote the integration windows used to calculate the mean coherences shown in *E* and *F*. For clarity, error bars are shown for only every other data point. *B*: coherence between the HSS neuron response and a preferred axis rotation, sideward and forward translation for the entire flight. We assumed the yaw axis as the preferred rotation axis of HS neurons. *C*: as in *A*, for the response in the periods between the saccades. *D*: coherence between the HSS neuron response and a preferred rotation, sideward and forward translation for the periods between the saccades. Coherences in *C* and *D* were calculated by masking out the saccadic part of the stimulus and the neuronal response (cf. METHODS). *E*: mean coherences of all VS neuron types for a preferred axis rotation and an upward/downward translation for the entire flight and between the saccades. Frequencies were averaged over a frequency band of 10 Hz, centered near the maximum coherence for each condition. *F*: mean coherences of all HS neuron types for preferred rotation (yaw), sideward translation, and forward translation for the entire flight and between the saccades. All coherences and mean coherences are averages over the right and left neurons (VS1, 5 neurons; VS2-3, 4 neurons; VS4-6, 8 neurons; VS7, 1 neuron; HSN, 9 neurons; HSE, 8 neurons; HSS, 9 neurons). Error bars show SE.

most sensitive to downward motion in the lateral visual field and considered as a detector for roll rotations (Fig. 1*C*; Karmeier et al. 2003, 2005; Krapp et al. 1998).

Similar conclusions can be drawn for HSS neurons (Fig. 1*E*, *bottom*). There is no clear and simple relationship between the membrane potential fluctuations evoked by naturalistic optic flow and any single self-motion parameter. Both HSS neurons are depolarized with respect to the resting potential for most of the time during the flight. Their responses appear to be strongly affected by those saccadic turns that lead to image displacements in the antipreferred direction of the neuron. During those rotations the neuron becomes hyperpolarized. Again, these findings obtained with naturalistic optic flow cannot easily be inferred from results and conclusions based on simple experimenter-defined stimuli. Here, HSS neurons were found to be depolarized by front-to-back motion (Fig. 1*A*) and inhibited by back-to-front motion. They are responsive to rotations of the animal around a vertical axis, but, additionally, they respond to translational optic flow occurring during forward and sideward motion of the animal (Hausen 1982b; Krapp et al. 2001).

Responses of similar complexity are obtained for all other VS and HS neurons that were tested. Because it is hardly

possible to infer which aspects of self-motion are encoded by VS and HS neurons under natural conditions just by looking at the complex neuronal responses, the data will be analyzed in a quantitative way.

VS neurons

RECEPTIVE FIELDS AND PREFERRED AXES OF ROTATION. Like the VS6 neuron (Fig. 1*E*) all VS neurons have been suggested, on the basis of experiments with simple motion stimuli, to analyze optic flow resulting from rotations of the animal's head around a specific axis located in the horizontal plane (Krapp et al. 1998). The preference of a given VS neuron for a specific rotation axis is mediated by the distribution of local directional motion sensitivities within its receptive field (Krapp et al. 1998). The receptive fields of VS neurons from one half of the brain cover large parts of the corresponding visual hemisphere, but the maximum sensitivities to downward motion are distributed from the frontal (VS1) to the caudal part of the visual hemisphere (VS10) (Fig. 1*A*; Farrow et al. 2005; Haag and Borst 2004; Hengstenberg et al. 1982; Krapp et al. 1998). We took advantage of the different spatial locations of the sensi-

tivity maxima when identifying VS neurons. We stimulated each recorded neuron with a dot moving up- and downward at different azimuthal positions from $-15°$ at the contralateral side to $120°$ at the ipsilateral side (resolution $15°$). A $0°$ angle corresponds to the frontal midline of the visual field; positive and negative angles refer to angular positions in the right and left visual field, respectively. Figure 2*A* shows the resulting spatial sensitivity distribution of a VS1 and a VS6 neuron, as determined by the difference between the responses to down- and upward motion of the dot. Both neurons show a clear sensitivity maximum, but respond to motion stimuli over a broad range of stimulus positions. We fitted a Gaussian function to the measured data and took the maximum of the fit as the sensitivity maximum of the neuron (arrows in Fig. 2*A*). The sensitivity maximum of the VS1 neuron was found at an azimuth close to $0°$, the maximum of the VS6 neuron close to $90°$. The sensitivity maxima of VS2 to VS5 are located between the maxima of VS1 and VS6 (Fig. 2*D*).

To determine the preferred rotation axes of the different VS neurons when stimulated with naturalistic optic flow, we calculated for each neuron the coherence rate between the neuronal responses and rotations around axes of varying elevation and azimuth (cf. METHODS and Fig. 2*B*). The *inset* in Fig. 2*B* shows, as an example, the coherence between a VS6 neuron's response and rotations around two rotation axes (roll axis: azimuth $0/180°$ and elevation $0°$, corresponding to the head frontal axis; pitch axis: azimuth $-90/90°$ and elevation $0°$, corresponding to the head transverse axis). The coherence quantifies, as a function of frequency, the similarity of a self-motion parameter (here either roll or pitch) and the self-motion parameter predicted from the response by the optimal linear filter. The coherence varies between zero (i.e., at frequencies where the parameters are not linearly related) and one (i.e., perfect prediction; see METHODS). The coherence rate is obtained by integrating over the coherence function (see METHODS) and is a convenient way to collapse the coherence function into a single number (van Hateren and Snippe 2001). Figure 2*B* shows the coherence rates between the response of a single VS6 neuron and head rotations around a range of rotation axes covering the entire visual sphere. As can also be inferred from the coherence functions in the *inset*, the coherence rate was high for rotations around the roll axis, but low for rotations around the pitch axis. The rotation axis (i.e., with azimuth and elevation given at $5°$ resolution) that gave the maximum coherence rate was used as an estimate for the preferred rotation axis of the VS6 neuron. These estimates were obtained for typically eight stimulus conditions (all combinations of normal and mirrored movies, original and NT stimulus version, and coherence of total or only intersaccadic response). The estimates of the preferred rotation axes of a certain neuron were averaged and the SE provided a measure of the error in the average. We show in Fig. 2*C* the azimuth and elevation of the preferred rotation axes for all VS neurons recorded in the experiments. The preferred rotation axes are distributed within an azimuthal range of $110°$ (between -25 and $85°$). The elevation varies little and is generally close to $0°$ (i.e., the horizontal plane). It should be noted that the preferred axes of rotation as determined on the basis of naturalistic optic flow are very similar to those predicted from experiments using experimenter-defined, local motion stimuli (Krapp et al. 1998, 2001).

Interestingly, the preferred axes of rotation of the different VS neurons are related to the location of their receptive fields, i.e., the region in the visual field where they are most sensitive to motion. The position of the sensitivity maximum of a VS neuron measured with the dot stimulus is almost orthogonal to the corresponding preferred rotation axis. The two characteristics show a linear relationship (Fig. 2*D*; slope of regression line -1.1).

For the following analysis, we classified the recorded VS neurons on the basis of their response characteristics and their preferred axes of rotation (Fig. 2*C*). The VS1 neuron has very distinctive response properties and could thus be classified unambiguously (Krapp et al. 1998). The preferred rotation axes of all recorded VS1 neurons were located in a small azimuthal range between 75 and $85°$ (five neurons analyzed). A second group of neurons had their preferred rotation axes located in an azimuthal range between 46 and $63°$ and could be distinguished unambiguously from VS1 neurons. We pooled these neurons in the group of VS2-3 neurons because VS2 and VS3 neurons have virtually identical receptive fields and preferred directions (Krapp et al. 1998) and could also not be distinguished by the orientation of their preferred axes (four neurons belonging to this group were analyzed in detail). Although VS4, VS5, and VS6 neurons show slightly different receptive-field structures (Krapp et al. 1998), they could not be distinguished unambiguously on the basis of the identification stimuli used here. Because the preferred rotation axes of this group of neurons very clearly differ from those of the VS2-3 neurons, they were pooled in the group VS4-6 (eight neurons of this group were analyzed in detail). A single neuron we recorded from had its preferred rotation axis at an azimuthal position of $-25°$. Because this neuron clearly differed in its sensitivity maximum as well as in its preferred rotation axis from the neurons of the VS4-6 group, we classified it as a VS7 neuron. Neurons with more caudally oriented receptive fields could not be stimulated adequately with the stimulus device. It should be noted that the conclusions drawn in this study do not depend on the classification scheme used here. Qualitatively the same conclusions can be drawn when all neurons are treated separately.

COHERENCE FOR NATURALISTIC STIMULI. To determine how well different self-motion parameters are represented by the time-dependent responses of individual VS neurons to naturalistic optic flow, we calculated the coherences for rotations around their respective preferred axis and for upward/downward translation. As an example, Fig. 3, *A* and *C* shows the mean coherences determined for neurons of the VS4-6 group. If the entire flight is taken into account (Fig. 3*A*), the coherence between the neuronal responses and the rotation around the preferred axis (i.e., approximately the roll axis; see Fig. 2*C*) is >0.1 between 5 and 35 Hz. Surprisingly, the coherence for the upward/downward translation is small, although all VS neurons respond well to constant velocity up- and downward motion (Hengstenberg 1982; Hengstenberg et al. 1982; Karmeier et al. 2003). This difference is understandable because during saccades the rotational velocities are usually much larger than the angular velocities resulting from upward/downward translation and thus dominate the overall optic flow. The situation is different for the intersaccadic intervals. Thus we calculated the coherences for rotations around the preferred
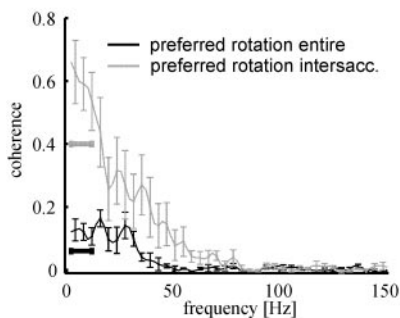
A VS4-6, NT-flight
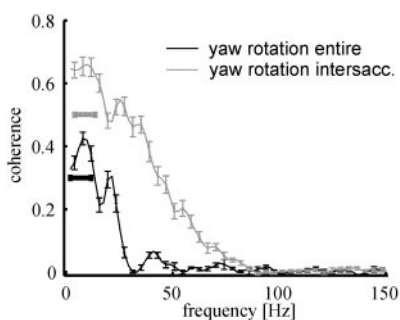
C NT-flight: VS-neurons

B HSN, NT-flight
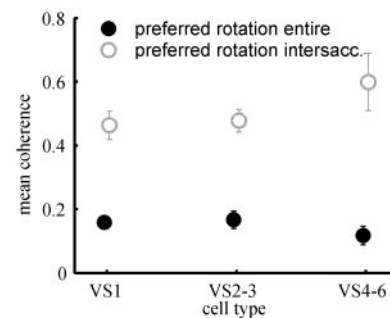
D NT-flight: HS-neurons
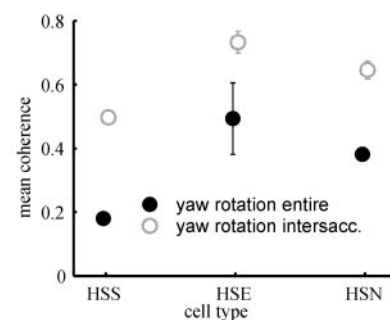
FIG. 4. Mean coherences between tangential neurons' responses and the "no translation" stimulus (NT). *A*: mean coherence of a neuron from the VS4-6 group neurons calculated for the rotation around the preferred axis for the entire NT flight and between the saccades (mean and SE). Horizontal bars in *A* and *B* denote the frequency range used to calculate the mean coherences shown in *C* and *D*. *B*: coherence between the HSN neurons' responses and yaw rotation for the entire flight and between the saccades. *C*: mean coherences for 3 groups of VS neurons calculated for the preferred rotation axis for the entire stimulus and between the saccades. *D*: mean coherences for the 3 HS neuron types calculated for yaw rotation for the entire NT stimulus and between the saccades. Mean coherences are averages over the right and left neuron (VS1, 5 neurons; VS2-3, 3 neurons; VS4-6, 4 neurons; HSN, 8 neurons; HSE, 2 neurons; HSS, 1 neuron). Error bars show SE.

axes and for upward/downward translation separately between saccades (Fig. 3*C*). The coherences for the intersaccadic velocities are higher and >0.1 between 1 and 35 Hz for both self-motion parameters. Thus it appears, in accordance with previous experiments done with experimenter-defined optic flow (Karmeier et al. 2003), that individual neurons of the VS4-6 group do not provide the information to easily distinguish between roll and upward/downward translation.

In Fig. 3*E* we compare for all groups of VS neurons the coherences for the preferred axes of rotation (cf. Fig. 2*C*) and for upward/downward translation. To combine all data in a single panel, we calculated the mean coherence by averaging the coherence functions over frequencies in a 10-Hz band around the frequency with maximum coherence (e.g., horizontal bars in Fig. 3, *A* and *C*). The mean coherences for rotations around the preferred axis and for upward/downward translation calculated for the entire flight are in the same range for all groups of VS neurons. Coherences >0.1 are obtained only for rotations. The coherences for the upward/downward translation were much smaller. In contrast to coherences for the entire flight, the coherences calculated for upward/downward translation in the intersaccadic intervals are >0.1 for all neuron groups. The coherences for the intersaccadic rotation velocities around the preferred axes differ between groups of VS neurons: The coherence for the intersaccadic rotation velocity is higher than the coherence for the entire flight for neurons of the VS4-6 and VS7 groups, although it decreases for neurons of the VS2-3 group and becomes almost negligible for VS1 neurons. This feature may be attributable to interference between the responses to rotation and translation.

This hypothesis is corroborated by results obtained with the NT stimulus (no translation; see METHODS), which allowed us to study the coding properties of VS neurons for rotations alone,

i.e., without simultaneous translational movements. The coherence function for the entire flights between preferred axis rotations and the neuronal responses shows similar values and frequency dependencies as the coherences of the original flight with simultaneous translations (compare Fig. 4, *A* and *C* to Fig. 3, *A*, *C*, and *E*). However, the coherences for the intersaccadic rotation velocities are higher than the coherences for rotation of the entire flight for all groups of VS neurons (Fig. 4*C*) and do not decrease at the lowest frequencies (Fig. 4*A*). The higher coherences between saccades are likely to be a consequence of the limited range in which the visual motion detection system encodes velocity linearly (Egelhaaf and Reichardt 1987; Haag and Borst 1997). We conclude from the comparison of the coherences obtained for the original and the NT flights that between saccades of normal flights, VS neurons carry information not only about rotation but also about upward/downward translation.

HS neurons

RECEPTIVE FIELDS AND THE "CLASSICAL VIEW". Like the HSS neuron shown in Fig. 1*D*, the other two types of HS neurons are also depolarized by front-to-back motion in the ipsilateral visual field, and all HS neurons were previously regarded as detectors of yaw rotations. The locations of the receptive fields differ between the three HS neurons. Whereas the sensitivity maximum of the HSS neuron is located in the ventral part of the visual field, the HSE neuron is most sensitive to motion in the equatorial and the HSN neuron in the dorsal part of the visual field. In addition to their main motion input in the ipsilateral visual field, HSN and HSE receive contralateral input from heterolateral connecting elements, in particular H1 and H2, that are sensitive to back-to-front motion (Haag and

Borst 2001; Hausen 1976, 1981, 1982b; Horstmann et al. 2000; Krapp et al. 2001). In an approach using naturalistic optic flow, Kern et al. (2005) concluded that the HSE neuron rather than primarily encoding yaw rotations of the animal also encodes information about sideward translation in the intersaccadic intervals. Here we show data for all three HS neurons. On the whole, the results for all HS neurons are similar, although there are characteristic differences that may be related to their different receptive locations and the presence or absence of contralateral input.

COHERENCE FOR NATURALISTIC STIMULI. For HS neurons we calculated the coherences between neuronal responses and the yaw rotation and those translations that can be expected to activate HS neurons, i.e., sideward and forward translation. Figure 3, *B* and *D* shows, as an example, the coherence functions calculated for HSS neurons. For the entire flight only the coherence of yaw velocity shows values >0.1 (between 1 and 15 Hz), whereas the coherences for both forward and sideward velocity are small (Fig. 3*B*). The coherence of the intersaccadic yaw and the sideward velocity are higher and have their maxima in adjacent frequency bands: Whereas the coherence of the intersaccadic yaw velocity and the neuronal response is >0.1 between about 20 and 60 Hz, the coherence of sideward velocity is high only at low frequencies ≤20 Hz (Fig. 3*D*). The mean coherences for all HS neurons, averaged over the frequency bands indicated by the horizontal bars in Fig. 3, *B* and *D*, are given in Fig. 3*F*.

For all HS neurons the intersaccadic yaw and sideward velocities were coded in different frequency bands as shown for the HSS neuron in Fig. 3*D*. HS neurons might make use of this difference to provide information on both optic flow components in adjacent (and thus separable) frequency bands (Kern et al. 2005). A comparable separation of information about rotational and translational components of self-motion is not possible for VS neurons, where rotation and translation are coded in similar frequency bands for both the entire flight and between the saccades (Fig. 3, *A* and *C*). Although the absolute coherence values obtained for the different HS neurons varied, possibly as a consequence of different average stimulus contrast in their receptive fields, they exhibited a similar relationship between the values obtained for the different self-motion parameters. In particular, the coherences between the neuronal responses and forward velocity were much smaller than those for sideward velocity.

If the translational components are eliminated from the optic flow, simulating pure rotations of the fly (NT-stimuli), it becomes obvious that, as in VS neurons, the translational component of self-motion had a substantial impact on the neuronal responses. For the entire NT flight the yaw coherence was larger than that for the original flight with translational components, but showed a similar frequency dependency (Fig. 4*B*, black line). If evaluated for the intersaccadic intervals the coherence function of the NT flights was also high in the low-frequency range, in contrast to the original flight (see also Kern et al. 2005). Similar to the VS neurons, all classes of HS neurons have a higher coherence between rotation and responses in intersaccadic intervals than for the entire flight (Fig. 4*D*).

Population coding

The coherence analysis of the responses of VS and HS neurons demonstrates that responses of single neurons carry significant, but partly ambiguous, information about self-motion. This gives rise to the question to what degree the combination of signals from different neurons can disambiguate the decoding. Two recent studies already demonstrated this improvement for tangential neurons: Kern et al. (2005) demonstrated that information of different parameters of self-motion can be separated by combining the responses of the ipsi- and contralateral HSE neurons. Karmeier et al. (2005) showed that the axis of self-rotation can be extracted with high accuracy from the population response of all VS neurons. As a first approach to analyzing population coding of naturalistic optic flow, we investigate linear combinations of neuronal signals and calculate the coherences with rotations around and translations along the three cardinal head axes (roll, pitch, and yaw; forward, sideward, and upward/downward). It should be noted that our analysis has limitations in addition to investigating linear combinations and focusing on orthogonal, cardinal axes. First, we did not record simultaneously from the various neurons, which implies that we cannot infer on possible correlations between the noise in the different neurons. Second, the neurons are generally recorded in different animals, which implies that possible correlations between the processing properties of different neurons in the same animal (e.g., through particularities of their common input elements) cannot be detected as well. For technical reasons, however, simultaneously recording from more than one of the HS and VS neurons with sufficient quality for a coherence analysis is extremely difficult. The approach we take here should therefore be considered as a first albeit feasible approach to the question how naturalistic, behaviorally generated optic flow is represented in the blowfly's brain.

CODING OF SELF-MOTION BY SUBPOPULATIONS OF VS NEURONS. The responses of individual VS neurons carry information about different rotation axes as well as about upward/downward velocity. We analyzed whether the specificity to self-rotation is enhanced by subtracting the responses of two sets of VS neurons from opposite halves of the brain having the same preferred rotation axis but opposite preferred rotation directions. In Fig. 5*A* we show the coherence function calculated between the intersaccadic roll velocity and a composite response. This composite response was obtained by subtracting the summated response of four ipsilateral neurons (three responses from three representative neurons of the VS4-6 group and one response from a VS7 neuron) from the summated four responses of the corresponding contralateral neurons. The coherence function was >0.1 between 1 and 50 Hz and shows a frequency dependency similar to that of the coherence calculated for the responses of individual VS4-6 neurons (cf. Fig. 3*C*). The coherence values, however, are larger than the values calculated for individual VS4-6 neurons. This is because more neuronal responses are incorporated in the analysis, which should increase the signal-to-noise ratio, and thus the coherence. The difference signal of a single VS4-6 neuron pair gives similar, but slightly lower coherences. This finding indicates that the exact grouping of VS neurons is not important with respect to the encoding of roll rotation. Because there is virtually no coherence between the difference signals and

A Roll rotation: VS4-7 difference signal

B Lift translation: VS1-7 summated signal

C Forward translation: HSS summated signal

D Sideward translation & yaw rotation: HSS difference signal
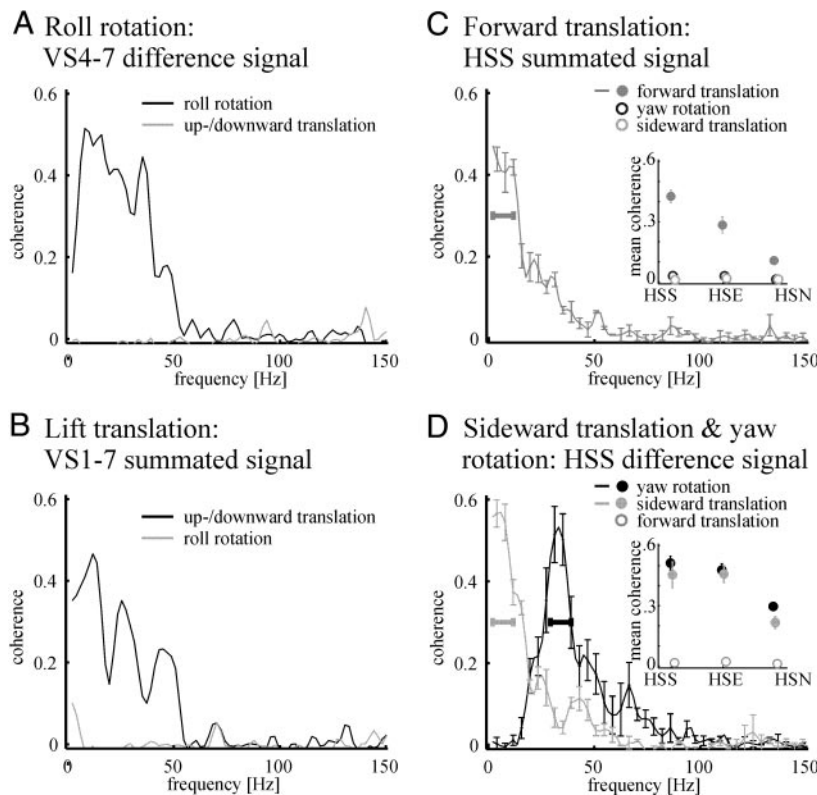
FIG. 5. Population coding of self-motion: coherences between cardinal self-motion components and the population response that leads to the highest coherence. *A*: coherence between intersaccadic roll rotation and a composite response obtained by subtracting the summated response of ipsilateral VS4-7 neurons from the summated 4 responses of the corresponding contralateral neurons (4 neuron pairs). Coherence between intersaccadic upward/downward velocity and the composite response is negligible. *B*: coherence between intersaccadic upward/downward velocity and the sum over 7 representative ipsilateral responses and the 7 corresponding contralateral responses from VS1-7 neurons (7 neuron pairs). Coherence between intersaccadic roll velocity and the summated response of ipsi- and contralateral VS1-7 neurons is negligible. *C*: coherence between the summated responses of the left and right HSS neuron and the intersaccadic forward velocity (average and SE of 3 HSS neurons). *Inset*: mean coherences of the summated response of the left and right neurons for all HS neurons (HSN, 9 neurons; HSE, 7 neurons; HSS, 3 neurons). Coherence was averaged over a 10-Hz window, centered near the maximum coherence. Coherences between the summated responses of the left and right HS neurons and yaw and sideward velocity is negligible for all 3 HS types. *D*: difference signal between the left and right HSS neurons produces high coherences with both intersaccadic yaw and sideward velocity (average of 3 HSS neurons). *Inset*: mean coherences of the difference signal for all HS neurons (HSN, 9 neurons; HSE, 7 neurons; HSS, 3 neurons). Coherences were averaged over 10-Hz windows. Coherence between the difference response of all 3 HS neuron types and forward velocity is negligible. All coherences were calculated for the intersaccadic intervals.

upward/downward velocity (Fig. 5*A*), taking the difference between VS neurons with opposite rotation sensitivities increases the specificity for rotational self-motion.

We could not obtain responses of VS10 neurons because the stimulus device does not allow us to stimulate neurons of this group that have their receptive fields in the rear part of the visual field. Because VS10 neurons were predicted on the basis of experimenter-defined stimuli to have approximately the same rotation axis as that of VS1 neurons but opposite preferred directions (Krapp et al. 1998), it is reasonable to hypothesize that subtracting the sum of the ipsi- and contralateral VS1 responses from the sum of the ipsi- and contralateral VS10 responses would yield a sizable and specific coherence with pitch.

Because all VS neurons respond to some extent to upward/downward translation, we tested whether the specificity for this translational component could be enhanced by an additive combination of all VS neurons. The coherence between the neuronal responses and upward/downward velocity was calculated from the signal obtained by summating the responses of representative neurons from all VS groups recorded in the experiments (seven neuronal responses from the ipsilateral side and seven neuronal responses from the contralateral side). Figure 5*B* shows that the coherence to upward/downward velocity was enhanced compared with single-neuron coherences by taking the responses of many VS neurons into account. The intersaccadic coherence to upward/downward velocity was >0.1 between 1 and 55 Hz and the peak coherence is considerably higher than that for individual VS neurons (between 0.1 and 0.2; see Fig. 3*E*). The coherences between the summated responses of VS neurons and different rotational self-motion components are negligible (Fig. 5*B*). Thus adding

the responses of a population of VS neurons increases the specificity for upward/downward translation.

POPULATION CODING IN HS NEURONS. The responses of all HS neurons carry information about yaw and sideward velocity. In a recent study, Kern et al. (2005) showed that the specificity of intersaccadic responses to translational self-motion components is enhanced by combining the responses of HSE neurons from both halves of the brain. Here we show that combining the responses of the ipsi- and contralateral neuron enhances the specificity of all HS neurons.

The coherence calculated between the summated signals of ipsi- and contralateral HSS neurons and forward translation is generally higher than the coherence calculated for the signal of individual HSS neurons (compare Figs. 5*C* and 3*F*). The values were >0.1 between 1 and 35 Hz. The coherence with yaw and sideward velocity (Fig. 5*C*, *inset*) is negligible in all three HS neurons, demonstrating that summation increases the specificity of these neurons to a single parameter of optic flow. The coherence with forward velocity was, of all HS neurons, highest for the HSS neuron (Fig. 5*C*, *inset*), which may be explained by both the absence of contralateral input to the HSS neuron and its sensitivity maximum in the ventral part of the visual field. The difference between the responses of corresponding ipsi- and contralateral HS neurons enhances the coherence for sideward and yaw velocities (Fig. 5*D*) and makes the coherence with forward velocity negligible (Fig. 5*D*, *inset*). As for the coherences calculated from the response of individual HS neurons (cf. Fig. 3*D*), information about sideward and yaw velocities is coded in adjacent frequency bands. The coherence for the difference response is larger for all types of HS neurons than the values calculated for individual HS neurons (cf. Fig. 5*D*, *inset*, and Fig. 3*F*).

DISCUSSION

Neuronal coding of visual motion has often been analyzed by characterizing single neurons with simple, experimenter-defined motion stimuli. This approach, however, is known to be artificial: The characteristic temporal structure of the visual input an animal experiences during unrestrained behavior differs dramatically from the experimenter-defined motion stimuli used in earlier studies, whether it is constant velocity stimuli or white-noise velocity fluctuations (e.g., David et al. 2004; Kern et al. 2005; van Hateren et al. 2005; Vinje and Gallant 2002). Furthermore, it is known that information is conveyed by neuronal populations rather than by single neurons (e.g., Fitzpatrick et al. 1997; Georgopoulos et al. 1986; Groh 2000; Lee et al. 1998; Nicolelis et al. 1998; Theunissen and Miller 1991; Zhang et al. 1998). Therefore the aim of this study was to analyze how self-motion is encoded by a population of blowfly visual interneurons stimulated with naturalistic optic flow as generated during free-flight behavior. We could demonstrate that by exploiting the specific dynamics of natural optic flow; the population response provides information about all six degrees of freedom of self-motion.

The responses of individual sensory neurons are usually highly ambiguous with respect to different stimulus parameters. This is also true for VS and HS neurons (Hausen 1982a,b; Hengstenberg 1982; Hengstenberg et al. 1982). Part of these ambiguities can be reduced when the neurons are stimulated with moving patterns that come close to natural scenes with regard to their statistical properties, i.e., which are composed of a broad range of spatial frequency components and contrasts (Dror et al. 2001). The results of Dror et al. (2001) are corroborated by the finding that during stimulation with naturalistic optic flow even large differences in the textural properties of the scene have little effect on the responses of fly motion-sensitive neurons. Rather, the neuronal responses are mainly shaped by the characteristic dynamical properties of the naturalistic optic flow (Boeddeker et al. 2005; Kern et al. 2005; Lindemann et al. 2005; van Hateren et al. 2005).

The specific dynamical properties of naturalistic optic flow are the consequence of a saccadic flight and gaze strategy of blowflies (Schilstra and van Hateren 1999; van Hateren and Schilstra 1999): Brief periods dominated by high rotation velocities, the saccades, are followed by periods characterized by almost stable gaze and thus much smaller rotational velocities. This aspect of the gaze strategy of blowflies is reminiscent of the saccadic eye movements of primates where the retinal image is stabilized by a pattern of fixations with interspersed fast saccades that shift the gaze direction to objects of interest (e.g., Becker 1992; Carpenter 1988). If blowflies are moving in a textured environment containing nearby objects, the optic flow in the intersaccadic intervals constitutes significant translational components and thus contains information about the spatial layout of the environment.

The relationship between the complex time-dependent responses of the analyzed HS and VS neurons and the different self-motion parameters is much more obvious only if the responses during the intersaccadic intervals are taken into account. If the entire flight is taken into account the responses evoked by the rotational self-motion components dominate those evoked by translational self-motion components and only the coherences for the rotational velocities are >0.1. If, in contrast, only the responses during the intersaccadic intervals are evaluated, the coherences to both the rotational and the translational components of optic flow reveal values >0.1. Therefore the blowfly's saccadic flight and gaze strategy can be interpreted as a means to separate actively rotational and translational optic flow components and thus facilitate the computation of behaviorally relevant information.

The computations that were used here to separate the saccadic and intersaccadic parts of the neuronal responses are used only for analytical purposes and not as a model of the neural processing. The nervous system is likely to use different strategies. One possible strategy would be to suppress or modify the neuronal response during saccades as has been shown for the saccadic system of primates (e.g., Bair and O'Keefe 1998; Burr 2004; Thiele et al. 2002), implicating signals derived from the saccadic control system. In blowflies, this kind of top-down modification of the neuronal representations of optic flow is apparently absent in VS and HS neurons because their responses to naturalistic optic flow appear to be exclusively driven by the visual stimulus. This is concluded from the close similarity between the responses of HS neurons and the output of a model of computational mechanisms implemented by the neuronal circuits in the blowfly motion vision pathway (Lindemann et al. 2005). Nonetheless, it is conceivable that top-down signals play a decisive role in separating the neuronal representation of natural optic flow into its saccadic and intersaccadic components at some later processing stage.

Although the dynamics of naturalistic optic flow shape the responses of VS and HS neurons, the responses of individual neurons are still ambiguous. Each VS neuron, for example, responds best to rotations about one axis located approximately in the equatorial plane of the head. Additionally each neuron represents information about upward/downward translation during the intersaccadic intervals. Similarly, in the intersaccadic intervals HS neurons provide information about yaw rotations, sideward translation, and, to some extent, forward translation. These ambiguities can be dramatically reduced by considering neuronal population activity. As predicted theoretically (e.g., Dahmen et al. 2000), the specificity for a particular axis of self-rotation of the animal can be enhanced by a subtractive combination of pairs of neurons with different preferred rotation axes. Subtraction of the outputs of heterolateral VS4-6 and VS7 neurons increases the specificity for rotations around the *roll* axis (Fig. 6A). Accordingly, specific representations of *yaw* rotations are obtained in a separable frequency band (see following text) by subtraction of the responses of ipsi- and contralateral HS neurons (Fig. 6B). Concerning the encoding of *pitch* rotations we can currently propose only a hypothesis because the probably involved VS10 neuron cannot be stimulated adequately by our visual stimulator. The only data available on the VS10 neuron are those based on simple experimenter-defined stimuli (Krapp et al. 1998). The measured preferred rotation axis of the VS1 and the predicted axis of the VS10 neuron correspond to the *pitch* axis, although with opposite directions. Just as the subtractive combination of the heterolateral VS4-6 and VS7 neurons enhances the specificity for rotations around the *roll* axis, the specificity for *pitch* rotation should be enhanced by subtracting the signals of VS1 and VS10 neurons (Fig. 6C).
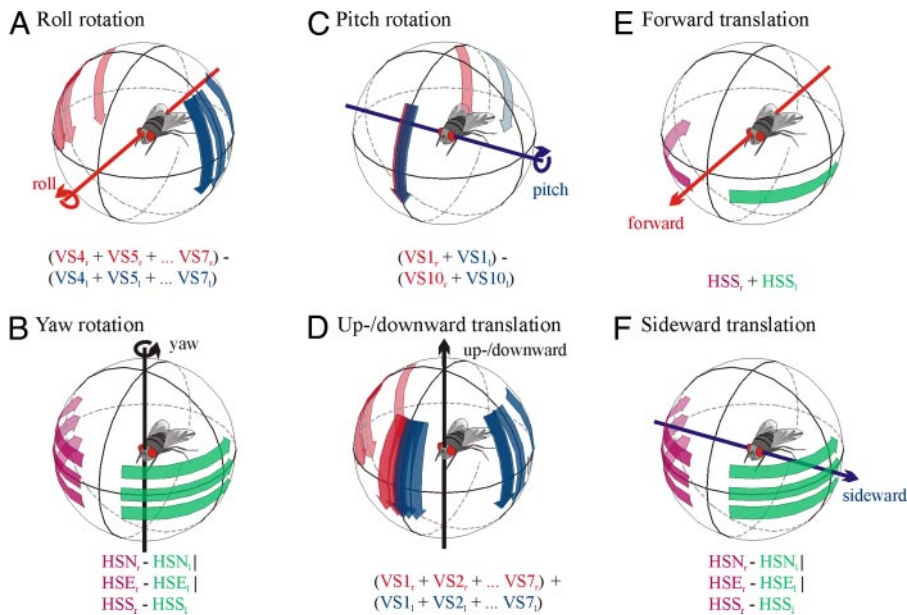
FIG. 6. Population coding of self-motion: neuronal populations appropriate for the encoding of self-motion around and along all 3 cardinal head axes. *A–C*: specificity to self-rotation is enhanced by subtracting the responses of 2 sets of neurons from opposite sides of the visual sphere having the same preferred rotation axis but opposite preferred rotation directions. *A*: subtracting responses of a group of heterolateral VS neurons with laterally located receptive fields increases the specificity to roll rotation. *B*: subtracting responses of heterolateral HS neuron pairs (HSN, HSE, and HSS) increases the specificity to yaw rotation. *C*: subtracting responses of VS neurons with frontally and caudally located receptive fields should increase the specificity to pitch rotation. *D–F*: specificity to self-translation is enhanced by summating responses of neurons exhibiting the same sensitivity or by subtracting neurons with opposite sensitivity to the respective self-motion. *D*: summating responses of all recorded VS neuron types enhances the specificity to up-/downward translation. *E*: summating responses of heterolateral HSS neurons with ventrally located receptive fields increases the specificity to forward translation. *F*: subtracting responses of heterolateral HS neuron pairs (HSN, HSE, and HSS) increases the specificity to sideward translation.

A specific representation of *upward/downward* translation is obtained by adding the responses of all VS neurons in both halves of the brain (Fig. 6*D*). In a similar way, the addition of the responses of heterolateral HS neurons isolates the information carried about *forward* translation (Fig. 6*E*). Interestingly, the specificity of the summated responses for forward translation decreases from the HSS by the HSE to the HSN neuron. This gradient may be explained by the fact that the HSS neuron has its sensitivity maximum in the ventral part of the visual field, which is well stimulated during forward motion. It may also be related to the different input organization of the HSS neuron compared with the HSE and HSN neurons. In contrast to the latter neurons, the HSS neuron does not receive input from the contralateral eye (Hausen 1982a,b; Krapp et al. 2001). Recovering information about sideward translation from naturalistic optic flow appears, at first sight, to be more complicated. *Sideward* translation can be recovered by subtracting the output signals of the corresponding HS neurons from both halves of the brain (Fig. 6*F*). However, this difference signal also provides information about *yaw* rotation (see above). Nonetheless, as was concluded in a previous study (Kern et al. 2005), sideward translation can be separated from yaw rotation because of the different frequency content of the self-motion components, reflected in the relatively high coherence in adjacent frequency bands. Therefore all six cardinal axes of self-motion can be read out in a relatively simple way from the population response of VS and HS neurons. Furthermore, combining responses of different neurons may reduce ambiguities arising from the neuronal variability in the responses of VS and HS neurons (e.g., Haag and Borst 2004; Warzecha and Egelhaaf 2001; Warzecha et al. 2003; Zohary et al. 1994).

Although specific representations of all six self-motion parameters are obtained by combining signals of various subpopulations of VS and HS neurons in a linear way, it is likely that combining responses in a more sophisticated way may lead to even more specific neuronal representations of self-motion. All schemes proposed can be considered as feasibility proofs, revealing that the population response of VS and HS neurons

contains behaviorally relevant information that can be extracted in well-defined ways. Other decoding schemes may well be realized in the real system. This limitation pertains to most systems where neuronal population activity has been analyzed and for most computational mechanisms suggested for decoding neuronal population responses (for review see Dayan and Abbott 2001; Pouget et al. 2003). Hitherto there are only few neuronal systems where the decoding of sensory population activity by downstream motor systems has been investigated. One example is the mechanosensory system of the leech controlling evasive bending movements of the animal (e.g., Garcia-Perez et al. 2005; Lewis and Kristan 1998; Zoccolan and Torre 2002; Zoccolan et al. 2002). There are also initial attempts to analyze how the population response of VS and HS neurons is decoded to control compensatory head movements (Huston and Krapp 2003). In addition, model simulations are used to test how HS neurons may steer a saccadic controller, allowing a model fly to navigate in complex environments (Lindemann et al., unpublished observations). Moreover, we could show in a recent study that the axis of self-rotation can be inferred by a Bayesian decoder (for review see Dayan and Abbott 2001) from the population response of VS neurons (Karmeier et al. 2005). It would be interesting to extend this analysis to population responses evoked by naturalistic optic flow stimuli.

In conclusion, the responses of output neurons of the blowfly's visual motion pathway are largely shaped by the specific dynamical properties of the fly's saccadic flight and gaze strategy. This strategy has been interpreted as a simple way to squeeze most of the rotational optic flow into saccades, leading to optic flow between saccades that contains a strong translational component (Kern et al. 2005). This is likely to be decisive from a functional perspective because only the translational optic flow component contains information about the spatial layout of the environment. To blowflies, optic flow is most likely the only relevant source of information about the spatial layout of the outside world. A large part of the output neurons of the blowfly's visual motion pathway thus seems to

be well adapted to extract behaviorally relevant information from optic flow.

REFERENCES

Averbeck BB and Lee D. Coding and transmission of information by neural ensembles. *Trends Neurosci* 27: 225–230, 2004.

Bair W and O'Keefe LP. The influence of fixational eye movements on the response of neurons in area MT of the macaque. *Vis Neurosci* 15: 779–786, 1998.

Becker W. Saccades. In: *Eye Movements*, edited by Carpenter RHS. London: Macmillan, 1992, p. 95–137.

Bendat JS and Piersol AG. *Random Data.* New York: Wiley–Interscience, 2000.

Boeddeker N, Lindemann JP, Egelhaaf M, and Zeil J. Responses of blowfly motion-sensitive neurons to reconstructed optic flow along outdoor flight paths. *J Comp Physiol A Neuroethol Sens Neural Behav Physiol* 191: 1143–1155, 2005.

Borst A and Haag J. Neural networks in the cockpit of the fly. *J Comp Physiol A Sens Neural Behav Physiol* 188: 419–437, 2002.

Burr D. Eye movements: keeping vision stable. *Curr Biol* 14: R195–R197, 2004.

Carpenter RHS. *Movements of the Eyes.* London: Pion, 1988.

Dahmen HJ, Franz MO, and Krapp HG. Extracting egomotion from optic flow: limits of accuracy and neural matched filters. In: *Computational, Neural and Ecological Constraints of Visual Motion Processing*, edited by Zanker JM and Zeil J. Berlin: Springer-Verlag, 2000.

David SV, Vinje WE, and Gallant JL. Natural stimulus statistics alter the receptive field structure of V1 neurons. *J Neurosci* 24: 6991–7006, 2004.

Dayan P and Abbott LF. *Theoretical Neuroscience: Computational and Mathematical Modeling of Neural Systems.* Cambridge, MA: MIT Press, 2001.

Deadwyler SA and Hampson RE. The significance of neural ensemble codes during behavior and cognition. *Annu Rev Neurosci* 20: 217–244, 1997.

Dror RO, O'Carroll DC, and Laughlin SB. Accuracy of velocity estimation by Reichardt correlators. *J Opt Soc Am A Opt Image Sci Vis* 18: 241–252, 2001.

Egelhaaf M, Grewe J, Karmeier K, Kern R, Kurtz R, and Warzecha A. Novel approaches to visual information processing in insects: case studies on neuronal computations in the blowfly visual motion pathway. In: *Methods in Insect Sensory Neuroscience*, edited by Christensen T. Boca Raton, FL: CRC Press, 2004.

Egelhaaf M, Kern R, Krapp HG, Kretzberg J, Kurtz R, and Warzecha AK. Neural encoding of behaviourally relevant visual-motion information in the fly. *Trends Neurosci* 25: 96–102, 2002.

Egelhaaf M and Reichardt W. Dynamic response properties of movement detectors: theoretical analysis and electrophysiological investigation in the visual system of the fly. *Biol Cybern* 56: 69–87, 1987.

Farrow K, Borst A, and Haag J. Sharing receptive fields with your neighbors: tuning the vertical system cells to wide field motion. *J Neurosci* 25: 3985–3993, 2005.

Fitzpatrick DC, Batra R, Stanford TR, and Kuwada S. A neuronal population code for sound localization. *Nature* 388: 871–874, 1997.

Franceschini N. *Sampling of Visual Environment by the Compound Eye of the Fly: Fundamentals and Applications.* Berlin: Springer-Verlag, 1975.

Garcia-Perez E, Mazzoni A, Zoccolan D, Robinson HPC, and Torre V. Statistics of decision making in the leech. *J Neurosci* 25: 2597–2608, 2005.

Georgopoulos AP, Schwartz AB, and Kettner RE. Neuronal population coding of movement direction. *Science* 233: 1416–1419, 1986.

Groh JM. Predicting perception from population codes. *Nat Neurosci* 3: 201–202, 2000.

Haag J and Borst A. Encoding of visual motion information and reliability in spiking and graded potential neurons. *J Neurosci* 17: 4809–4819, 1997.

Haag J and Borst A. Active membrane properties and signal encoding in graded potential neurons. *J Neurosci* 18: 7972–7986, 1998.

Haag J and Borst A. Recurrent network interactions underlying flow-field selectivity of visual interneurons. *J Neurosci* 21: 5685–5692, 2001.

Haag J and Borst A. Neural mechanism underlying complex receptive field properties of motion-sensitive interneurons. *Nat Neurosci* 7: 628–634, 2004.

Hausen K. Functional characterization and anatomical identification of motion sensitive neurons in the lobula plate of the blowfly *Calliphora erythrocephala. Z Naturforsch* 31c: 629–633, 1976.

Hausen K. Monocular and binocular computation of motion in the lobula plate of the fly. *Verh Dtsch Zool Ges* 74: 49–70, 1981.

Hausen K. Motion sensitive interneurons in the optomotor system of the fly. I. The horizontal cells: structure and signals. *Biol Cybern* 45: 143–156, 1982a.

Hausen K. Motion sensitive interneuron in the optomotor system of the fly. II. The horizontal cells: receptive field organization and response characteristics. *Biol Cybern* 46: 67–79, 1982b.

Hengstenberg R. Common visual response properties of giant vertical cells in the lobula plate of the blowfly Calliphora. *J Comp Physiol A Sens Neural Behav Physiol* 149: 179–193, 1982.

Hengstenberg R, Hausen K, and Hengstenberg B. The number and structure of giant vertical cells (VS) in the lobula plate of the blowfly Calliphora erythrocephala. *J Comp Physiol A Sens Neural Behav Physiol* 149: 163–177, 1982.

Horstmann W, Egelhaaf M, and Warzecha AK. Synaptic interactions increase optic flow specificity. *Eur J Neurosci* 12: 2157–2165, 2000.

Huston S and Krapp HG. The visual receptive field of a fly neck motor neuron. In: *Proceedings of the 29th Göttingen Neurobiology Conference*, edited by N. Elsner and Zimmermann H. New York: Thieme, 2003.

Johnston D and Wu MS. *Foundations of Cellular Neurophysiology* Cambridge, MA: MIT Press, 1995.

Karmeier K, Krapp HG, and Egelhaaf M. Robustness of the tuning of fly visual interneurons to rotatory optic flow. *J Neurophysiol* 90: 1626–1634, 2003.

Karmeier K, Krapp HG, and Egelhaaf M. Population coding of self-motion: applying bayesian analysis to a population of visual interneurons in the fly. *J Neurophysiol* 94: 2182–2194, 2005.

Kern R, van Hateren JH, Michaelis C, Lindemann JP, and Egelhaaf M. Function of a fly motion-sensitive neuron matches eye movements during free flight. *PLoS Biol* 3: e171, 2005.

Krapp HG, Hengstenberg B, and Hengstenberg R. Dendritic structure and receptive-field organization of optic flow processing interneurons in the fly. *J Neurophysiol* 79: 1902–1917, 1998.

Krapp HG, Hengstenberg R, and Egelhaaf M. Binocular contributions to optic flow processing in the fly visual system. *J Neurophysiol* 85: 724–734, 2001.

Lee D, Port NL, Kruse W, and Georgopoulos AP. Variability and correlated noise in the discharge of neurons in motor and parietal areas of the primate cortex. *J Neurosci* 18: 1161–1170, 1998.

Lewis JE and Kristan WB. A neuronal network for computing population vectors in the leech. *Nature* 391: 76–79, 1998.

Lindemann JP, Kern R, Michaelis C, Meyer P, van Hateren JH, and Egelhaaf M. FliMax, a novel stimulus device for panoramic and high-speed presentation of behaviourally generated optic flow. *Vision Res* 43: 779–791, 2003.

Lindemann JP, Kern R, van Hateren JH, Ritter H, and Egelhaaf M. On the computations analyzing natural optic flow: quantitative model analysis of the blowfly motion vision pathway. *J Neurosci* 25: 6435–6448, 2005.

Nicolelis MA, Ghazanfar AA, Stambaugh CR, Oliveira LM, Laubach M, Chapin JK, Nelson RJ, and Kaas JH. Simultaneous encoding of tactile information by three primate cortical areas. *Nat Neurosci* 1: 621–630, 1998.

Nirenberg S and Latham PE. Population coding in the retina. *Curr Opin Neurobiol* 8: 488–493, 1998.

Pouget A, Dayan P, and Zemel R. Information processing with population codes. *Nat Rev Neurosci* 1: 125–132, 2000.

Pouget A, Dayan P, and Zemel RS. Inference and computation with population codes. *Annu Rev Neurosci* 26: 381–410, 2003.

Reinagel P. How do visual neurons respond in the real world? *Curr Opin Neurobiol* 11: 437–442, 2001.

Schilstra C and van Hateren JH. Blowfly flight and optic flow. I. Thorax kinematics and flight dynamics. *J Exp Biol* 202: 1481–1490, 1999.

Stavenga D, Schwering P, and Tinbergen J. A three-compartment model describing temperature changes in tethered flying blowflies. *J Exp Biol* 185: 326–333, 1993.

Theunissen F, Roddey JC, Stufflebeam S, Clague H, and Miller JP. Information theoretic analysis of dynamical encoding by four identified primary sensory interneurons in the cricket cercal system. *J Neurophysiol* 75: 1345–1364, 1996.

Theunissen FE and Miller JP. Representation of sensory information in the cricket cercal sensory system. II. Information theoretic calculation of system

accuracy and optimal tuning-curve widths of four primary interneurons. *J Neurophysiol* 66: 1690–1703, 1991.

Thiele A, Henning P, Kubischik M, and Hoffmann K-P. Neural mechanisms of saccadic suppression. *Science* 295: 2460–2462, 2002.

van Hateren JH, Kern R, Schwerdtfeger G, and Egelhaaf M. Function and coding in the blowfly H1 neuron during naturalistic optic flow. *J Neurosci* 25: 4343–4352, 2005.

van Hateren JH, Ruttiger L, Sun H, and Lee BB. Processing of natural temporal stimuli by macaque retinal ganglion cells. *J Neurosci* 22: 9945–9960, 2002.

van Hateren JH and Schilstra C. Blowfly flight and optic flow. II. Head movements during flight. *J Exp Biol* 202: 1491–1500, 1999.

van Hateren JH and Snippe HP. Information theoretical evaluation of parametric models of gain control in blowfly photoreceptor cells. *Vision Res* 41: 1851–1865, 2001.

Vinje WE and Gallant JL. Natural stimulation of the nonclassical receptive field increases information transmission efficiency in V1. *J Neurosci* 22: 2904–2915, 2002.

Warzecha A and Egelhaaf M. Neuronal encoding of visual motion in real-time. In: *Motion Vision—Computational, Neural, and Ecological Constraints*, edited by Zeil J and Zanker J. New York: Springer-Verlag, 2001.

Warzecha A, Kurtz R, and Egelhaaf M. Synaptic transfer of dynamic motion information between identified neurons in the visual system of the blowfly. *Neuroscience* 119: 1103–1112, 2003.

Warzecha AK, Egelhaaf M, and Borst A. Neural circuit tuning fly visual interneurons to motion of small objects. I. Dissection of the circuit by pharmacological and photoinactivation techniques. *J Neurophysiol* 69: 329–339, 1993.

Zhang K, Ginzburg I, McNaughton BL, and Sejnowski TJ. Interpreting neuronal population activity by reconstruction: unified framework with application to hippocampal place cells. *J Neurophysiol* 79: 1017–1044, 1998.

Zoccolan D, Pinato G, and Torre V. Highly variable spike trains underlie reproducible sensorimotor responses in the medicinal leech. *J Neurosci* 22: 10790–10800, 2002.

Zoccolan D and Torre V. Using optical flow to characterize sensory-motor interactions in a segment of the medicinal leech. *J Neurosci* 22: 2283–2298, 2002.

Zohary E, Shadlen MN, and Newsome WT. Correlated neuronal discharge rate and its implications for psychophysical performance. *Nature* 370: 140–143, 1994.